Chemico-Biological Interactions 250 (2016) 27–37

Contents lists available at ScienceDirect

Chemico-Biological Interactions

journal homepage: www.elsevier.com/locate/chembioint

Murine breast carcinoma 4T1 cells are more sensitive to atranorin than normal epithelial NMuMG cells *in vitro*: Anticancer and hepatoprotective effects of atranorin *in vivo*

Peter Solár [a, *], Gabriela Hrčková [b], Lenka Koptašíková [a], Samuel Velebný [b], Zuzana Solárová [c], Martin Bačkor [a]

[a] Institute of Biology and Ecology, Faculty of Science, P.J. Šafárik University in Košice, 040 01 Košice, Slovak Republic
[b] Parasitological Institute of the Slovak Academy of Sciences, 040 01 Košice, Slovak Republic
[c] Institute of Pharmacology, Faculty of Medicine, P.J. Šafárik University in Košice, 040 01 Košice, Slovak Republic

ARTICLE INFO

Article history:
Received 28 November 2015
Received in revised form
9 February 2016
Accepted 7 March 2016
Available online 8 March 2016

Keywords:
Lichen
Atranorin
4T1 breast cancer
NMuMG cells
BALB/c mouse
Lipid peroxidation

ABSTRACT

The aim of this study was to evaluate the anticancer effect of atranorin (ATR) on murine 4T1 breast carcinoma cells and compare its sensitivity with normal mammary epithelial NMuMG cells *in vitro*. Antitumor and hepatoprotective activity of ATR-therapy was examined on mouse model of 4T1-induced cancer disease. ATR significantly reduced clonogenic ability of carcinoma 4T1 cells at the concentration of 75 μM, but clonogenicity of normal NMuMG cells was not affected by any of ATR concentrations tested. Moreover, flow cytometric and BrdU incorporation analysis did not confirm the inhibited entry into S-phase of the cell cyle after ATR incubation, and on the contrary, it induced apoptosis associated with the activation of caspase-3 and PARP cleavage in 4T1 cells. Although ATR did not cause any significant changes in Bcl-x_L protein expression in NMuMG cells, an apparent depletion of Bcl-x_L protein in 4T1 cells after 48 h ATR therapy was confirmed. Based on this result as well as the result of the total cell number decline, we can conclude that 4T1 cells are more sensitive to ATR therapy than NMuMG cells. ATR administration resulted in significantly longer survival time of BALB/c mice inoculated with 4T1 cells, what was associated with reduced tumor size and the higher numbers of apoptotic 4T1 cells. No differences were recorded in the number of BrdU-positive tumor cells between ATR-treated group and controls. Results indicate that ATR has rather proapoptotic than antiproliferative effect on 4T1 cells *in vitro* and *in vivo* and normal NMuMG cells are less sensitive to ATR. Furthermore, our studies revealed protective effect of ATR against oxidative stress in the livers of the tumor-bearing mice.

1. Introduction

Nowadays, the power of lichen extracts comes into consideration, while in natural medicine [7] it has been known for a long period of time. Lichens have been used for medicinal purposes throughout the ages [34] and some species, such as *Cetraria islandica*, *Lobaria pulmonaria* and *Cladonia species* were reputed to be effective in the treatment of pulmonary tuberculosis [54], even though their secondary metabolites are usually toxic to humans at the higher concentrations.

Lichen secondary metabolites putatively protect lichens from a variety of environmental stress factors [53] and harmful light irradiation [38]. Lichens produce several classes of phenolic compounds, including: depsides, depsidones, dibenzofuranes, xanthones, and anthraquinones [24]. Most of the secondary metabolites are formed as a part of the acetate-polymalonate biosynthetic pathway, but can also be produced by mevalonic acid and the shikimic acid pathways. Secondary metabolites are produced by the fungus alone and secreted onto the surface of lichen's hyphae either in amorphous forms or crystal form [55]. Although there are hundreds of lichens secondary metabolites, their particular functions are almost unknown.

Natural product atranorin (ATR) isolated from lichens is classified as depside based on the presence of its a *2,4-dihydroxy-3-aldehyde-6-methylbenzoate* moiety [15]. Except of ATR, other important members of the depside group are fumarprotocetraric

* Corresponding author. Moyzesova 11, 040 01 Košice, Slovak Republic.
E-mail address: peter.solar@upjs.sk (P. Solár).

http://dx.doi.org/10.1016/j.cbi.2016.03.012
0009-2797/

acid and gyrophoric acid. ATR is a colourless pigment [49] representing a major secondary compound found in the cortical layer of *Parmelia sulcata* [41], in the hyphae of *H. physodes*, *Cladina* and *Flavocetraria* sp. [18], *Parmotrema stuppeum* [53], *Stereocaulon alpinum* [25], *Physcia aipolia* [49] and many others [7,29,47].

ATR activities have not been studied in a detail and little information regarding its biological activities [25] is available in the literature published so far. Except for its antimicrobial properties, ATR has a wide variety of biological actions such as antiherbivorous [36], antiviral (inhibition of HIV virus replication) [13,23], elastase- [43] and trypsin-inhibiting [7] actions, analgesic and anti-inflammatory properties [10,19], potential immune-modulating properties [12], antinociceptive activities in the acute model of inflammation [29,33,47] spasmolytic effects [29], antioxidant activity *in vitro* [47] and superoxide scavenger activities [34].

Currently, only basic cancer research *in vitro* has been carried out to evaluate the potential anticancer and antiproliferative properties of the most known lichen metabolites as well as its extracts. The effect of usnic acid against cancer cells was originally noted more than 30 years ago. Unfortunately, the literature was lacking more precise information about the mechanism of action [51]. Recently, cytotoxic or antiproliferative (antimitotic) and pro-apoptotic effects of usnic acid *in vitro* on human breast, ovarian, cervix, vulvar, colon, prostate, pancreatic, lung, mesothelioma, glioblastoma and leukemia cancer cell lines [1,2,6,9,11,17,32] was shown by the mechanism not related to alterations in the formation and/or stabilization of microtubules [39]. The cytotoxicity of usnic acid towards cancer cells can be improved by conjugation with polyamine chain [5]. Paradoxically, usnic acid was the most cytotoxic on the normal rat hepatocytes *in vitro* among 15 different lichen compounds tested [14].

Except for the most frequently studied lichen metabolite usnic acid, there are another secondary compounds with anticancer effects *in vitro*. In this regard, the activities of ATR [1,2,46], protolichesterinic acid [9,21,40,46], gyrophoric acid [1,2,11], vicanicin [9,46], lobaric acid [9,40], orcinol derivatives of tenuiorin [26], sphaerophorin, pannarin, and epiphorellic acid-1 [44,45] and others [6,8,11,28,52] have been demonstrated.

So far cancer research has been carried out to evaluate the potential anticancer and antiproliferative properties of the most frequently occurring lichen secondary metabolites. ATR activities have not been studied in details and there is a lack of information in the literature published so far about its anticancer and antiproliferative activities *in vivo*. The main goal of our work was to evaluate the potential mechanisms involved in anticancer effect of ATR on murine breast carcinoma cell line 4T1 in *in vitro* conditions and in tumor-bearing mice, as well as to compare the sensitivity of 4T1 cells versus normal NMuMG epithelial cells derived from murine mammary gland. Moreover, the hepatotoxicity of ATR after oral administration to mice was determined at the extent of lipid peroxidation.

2. Material and methods

2.1. Cell lines and atranorin

Both murine mammary carcinoma 4T1 and normal murine mammary gland NMuMG cell lines were obtained from the American Type Culture Collection (ATCC, Manassas, VA, USA). Cancer 4T1 cell line was grown in RPMI 1640 medium (Thermo Fisher Scientific, Waltham, MA, USA) enriched by 5 mm glutamate and 10% heat-noninactivated fetal bovine serum (FBS, Thermo Fisher Scientific) and maintained in a humidified incubator at 37 °C in an atmosphere of 5% CO_2. All media were gentamicin- and antiobiotics-free. Normal NMuMG cell line was cultured in Dulbecco's modified Eagle's minimal essential medium (DMEM; Sigma-Aldrich, St.Louis, MA, USA) containing 3.7 g/L NaHCO3, 4.5 g/L D-glucose, stable glutamine, 10% FBS noninactivated by heat (Thermo Fisher Scientific), supplemented with human insulin (57 μL/20 mL) (Humulin®R 100IU/mL, Lilly, Czech Republic). All culture media were antibiotics-free and both cell lines were used for experiments between 20th and 24th passages.

ATR (A6652, Sigma-Aldrich) for *in vitro* experiments was dissolved in DMSO (stock solution of 58 mM), aliquoted and stored at −80 °C. Stock solution of ATR was further diluted in culture medium to obtain the desired concentrations. The proportion of solvent DMSO in the culture media did not exceed 0.1%. This concentration of DMSO has been shown to have no effect on cell proliferation for both cell lines (data not shown). ATR for *in vivo* experiments was solubilized in food oil (4% suspension of cremophore oil in water), a vehiculum suitable for oral application of insoluble drugs.

2.2. Total cell number and the viability assay

Cells were seeded into 6 cm Petri dishes as follows: 4T1 cells at the concentration of 1×10^5 cells in complete RPMI-1640 medium; NMuMG cells at concentration of 2×10^5 in complete DMEM medium supplemented with human insulin (57 μl/20 ml). After allowing cells to adhere, ATR was added at the final concentrations of 25, 50 and 75 μM. After 24 h, 48 h and 72 h intervals the cells were washed once with PBS, harvested by trypsinization and then centrifuged. Finally, the cells were resuspended in PBS, stained with 0.5% eosin and counted in Bürker chamber by light microscopy. The viability of 4T1 and NMuMG cells was calculated according to the formula: % viability = (number of unstained cells counted/total number of cells counted) * 100.

2.3. Clonogenic assay

Cell survival was measured by colony formation assay. For clonogenic assays, 4T1 and NMuMG cells gained from the total cell number and the viability assay after 24 h incubation with various concentrations of ATR were plated in six-well tissue culture plates at the density of 1000 cells per well in complete media and cultured for another 8–10 days. Then, the media were removed, colonies were washed twice with cold PBS and stained with 0.1% methylene blue dye in 80% methyl alcohol. The number of colonies containing at least 50 cells was determined, and the surviving fractions were calculated using Clono-counter software [37]. The results of the clonogenic assay are presented as means ± SD of three independent experiments performed in duplicates.

2.4. Analysis of the cell-cycle distribution

Cell cycle analysis was performed as described by Solar et al. [48] and Bačkorova et al. [1]. The distribution of cells at different stages in the cell cycle was estimated by flow cytometric DNA analysis. Adherent cells were harvested by trypsinization 24, 48 or 72 h after treatment, then washed twice with cold phosphate-buffered saline (PBS) and subsequently fixed in 70% ice cold ethanol and stored at −20 °C for at least 24 h. Fixed cells were centrifuged, washed with PBS, stained with staining solution (20 μg/mL propidium iodide, 137 μg/mL RNase A and 0.1% Triton X-100 in PBS) in the dark for 30 min and measured with a flow-cytometer (FACSCalibur, Becton Dickinson, San Diego, CA, USA). For each sample, a minimum of 15,000 gated events was evaluated and analyzed with ModFit LT 3.0 software (Verity Software House, Topsham, ME, USA).

2.5. Proliferation test based on BrdU incorporation in vitro

Proliferation activity of cancer 4T1 cells was analyzed after 24, 48, and 72 h of ATR treatment using Cell proliferation ELISA, BrdU (colorimetric) assay Kit (Roche Applied Science, UK) according to the manufacturer's instructions. 4T1 cells were seeded into 96-well plates at the density of 1000 cells per well. After allowing cells to adhere (24 h), fresh medium containing ATR at various final concentrations (50, 100 and 150 μM) were added to each well and incubated for 18 h. Then cells were labelled with BrdU (10 μL/100 μL of complete media) for further 4 h and reactions were terminated after removing labeling medium. FixDenat solution (200 μL/well) was added to the wells for 30 min at RT and after washing step cell lysates were incubated with anti-BrdU-POD antibody for 90 min. Then the cells were washed three-times and the TMB substrate was added (100 μL/well) for 30 min. The absorbance was read at 620 nm in FluoStar Optima reader (BMG Labtechnologies GmbH, Offenburg, Germany). The results were evaluated as percentage (%) of BrdU incorporation in untreated control (100%) and presented as means (±SD) of three independent experiments performed in duplicates.

2.6. Caspases activation assay

Activity of caspase-3 in 4T1 and NMuMG cells was analyzed at 1, 3, and 6 h after ATR treatment (25 μM and 50 μM) using EnzChek® Caspase-3 Assay Kit (Molecular Probes, Waltham, MA, USA) according to the manufacturer's instructions. Cells were harvested by scraping, washed once in cold PBS and centrifuged. The cell pelets were incubated at 4 °C for 30 min in lysis buffer containing 200 mM TRIS, pH 7.5, 2 M NaCl, 20 mM EDTA, 0.2% TRITON X-100, diluted in dH_2O. The lysed cells were centrifuged at 5000 rpm for 5 min at 4 °C, and the supernatants were analyzed immediately according to the procedure described in the manufacturer's protocol. The Ac-DEVD-CHO inhibitor was used to confirm that the observed fluorescence signal in both induced and control cell populations is due to the activity of caspase-3 like proteases. The supernatans were incubated with inhibitor for 10 min at RT and remaining samples were stored on ice. Then no-inhibitor samples and inhibitor-containing samples were incubated with working solution of 5 mM Z-DEVD-R110 substrate diluted in 2× reaction buffer (50 mM PIPES, pH 7.4, 10 mM EDTA, 0.5% CHAPS; 1 M DTT (dithiothreitol), in dH_2O) for 30 min at RT and the fluorescence (excitation/emission ~ 496/520 nm) using FluoStar Optima reader (BMG Labtechnologies, GmbH) was analyzed. The results were expressed as proportion (%) of activity in untreated control, and presented as means (±SD) of three independent experiments performed in duplicates.

2.7. Western blotting

The expression of Bax, Bcl-xL, Hsp90, and PARP proteins, was evaluated by western blot analysis as described by Solar et al. [48]. Briefly, 4T1 and NMuMG cells were seeded and cultivated in 60 mm Petri dishes followed by ATR treatment for 24 and 48 h. Cells were then scrapped into ice-cold PBS and collected together with floating cells from culture media, washed twice in ice-cold PBS and lysed in lysis buffer. Protein concentration was determined by Lowry protein assay (BioRad Laboratories Inc., Hercules, CA, USA) and proteins (70 μg) were then separated on 12% SDS–polyacrylamide gel and transferred onto nitrocellulose membrane (Millipore, Bedford, MA, USA). After 30 min of membrane blocking at RT in 5% non-fat milk, the nitrocellulose membrane blots were incubated overnight at 4 °C with a primary antibody as follows: anti-Bax (SC-493, 1:200, Santa Cruz Biotechnology, CA, USA), anti- Bcl-xL (SC-1041, dilution 1:100, Santa Cruz Biotechnology), anti-PARP (SC-7150, 1:200, Santa Cruz Biotechnology), anti-Hsp90 (ALX-804-808, 1:1000, Alexis Biochemical, San Diego, CA, USA) and anti-β-actin (A5441, 1:5000, Sigma Aldrich). After washing steps, membranes were incubated for 1 h at RT with an appropriate horseradish-conjugated secondary antibody (goat anti-rabbit IgG F(AB′) 2, 1:10,000, PI-31461; goat anti-mouse IgG F(AB′) 2, 1:10,000, PI-31436 (Pierce, Rockford, IL, USA). Detection of antibody reactivity was performed with a chemiluminescence detection kit ECL+ (Pierce) and visualized on X-ray films (Foma Slovakia, Skycov, Slovakia). Equal sample loading was verified by immunodetection of β-actin. The densitometry of proteins was evaluated using the ELLIPSE software version 2.0.7.1 (ViDiTo, SR) and their relative density was calculated based on the density of the β-actin bands in each sample. Values were expressed as arbitrary densitometric units corresponding to signal intensity.

2.8. Animals, experimental design and 4T1 inoculation

The female of BALB/c mice were inoculated at the age of 10 weeks with 2.5×10^5 4T1 cells per animal into the fifth left mammary gland during short-term anesthesia (Narkamon, Rometar, Bioveta, CR). Subsequently, mice were divided into two groups: untreated control and ATR-treated group, both comprising 30 mice per group. The experiment was carried out according to the principles described by the Law No. 23/2009 of the Slovak Republic for the Care and Use of Laboratory Animals and approved by the ethic committee of the State Veterinary Administration of Slovak Republic. Growth of tumors was monitored from third day after 4T1 cells inoculation and the size of palpated tumors for each mouse was recorded individually. ATR suspension was administered orally at the dose of 30 mg/kg of body weight (in total volume of 0.2 ml) daily for 10 days, starting from day four after 4T1 cells inoculation. Next day following termination of the therapy (15 days after 4T1 inoculation), 10 animals from each group were killed and tumors and livers were isolated for the evaluation of anticancer and hepatotoxic/hepatoprotective effects of ATR. In addition, intact mice ($n = 5$) were treated with the same dosage of ATR for ten days and the livers were used to reveal the potential hepatototoxicity of ATR *in vivo*. Liver samples were frozen immediately at −80 °C for determination of lipid peroxides. The weight, width and length of tumors were measured and then processed for histological analyses. The remaining 20 animals in each group were used for evaluation of the survival rates by recording dead animals daily. Survival data were analyzed by the program MedCalc (http://www.medcalc.org/manual/kaplan-meier.php) as well as by GraphPad Prism Software (version 5) (GraphPad Software, Inc., SanDiego, CA, USA) and are presented in the Kaplan-Meier survival curves. Tumor volumes were calculated according to the formula: $V\ (cm^3) = (\pi \times s12) \times s_2/12$, where $s_1 < s_2$. The experiment was repeated twice.

2.9. Detection of BrdU on frozen tumor sections

To evaluate the antiproliferative potential of ATR *in vivo*, four mice from control and treated groups received one dose of BrdU solution (sterile PBS, pH 7.2, 0.2 ml/mouse) intraperitoneally at the concentration of 5 mg/kg of body weight 24 h before termination of the experiment and together with 10th dose of ATR. After killing the animals, isolated livers were used for biochemical analyses. Tumors were measured and then processed for the preparation of frozen sections. For the tissue cryoprotection, tumors were soaked for 1 h in cold *n*-heptane at 4 °C, washed in PBS and snap-frozen at −20 °C. Sections (10 μm thick) were prepared on Cryocut 1800 (Leica, Charleston, SC, USA) and used for the immunohistochemical detection of BrdU in proliferating 4T1 cells according to the procedure described by the antibody manufacturer (anti-BrdU-FITC,

#11170376001, Roche Diagnostics, Mannheim, Germany). Antibodies were diluted 1:100 in PBS containing 0.1% BSA and 1% goat serum and incubated for 60 min at RT. Subsequently, the sections were washed three times with PBS and mounted on slides.

2.10. Histology and immunohistochemistry on paraffin sections of tumors

2.10.1. Tissue processing

Tumors isolated from six animals without BrdU injection from both experimental groups of mice were fixed for 24 h in 4% paraformaldehyde (PFA) in PBS (pH 7.2) at 4 °C. Tumors were then washed under running tap water for about 6 h and processed according to the standard protocol used for paraffin histology. Tumors were embedded in low melting wax (Paraplast, Sigma-Aldrich) and 7 μm sections were cut. The slides were subsequently used in a set of staining protocols. Primarily, sections were stained with Mayer's haematoxylin/eosin following a standard protocol to visualise basic histomorphology. After dehydration step in a set of graded alcohols and incubation in Histochoice clearing solution (Amresco, Solon, OH, USA), sections were mounted into permanent transparent medium Histochoice mounting fluid (Amresco).

2.10.2. Detection of apoptosis using immunohistochemistry

A part of histological sections was stained with Mayer's haematoxylin and eosin to describe the general morphology of mammary gland tumors. Detection of cells expressing markers of apoptotic process was performed by immunohistochemical localization of pro-apoptotic protein Bax and anti-apoptotic protein Bcl-x_L. Rehydrated sections were washed in distilled water followed by unmasking of antigenic epitopes. This was performed in boiling citrate buffer (pH 6.0) for 10 min. Then the sections were incubated with following primary antibodies: anti-Bax (rabbit monoclonal; dilution 1:300; Cell Signaling, CA, USA), anti-Bcl-x_L (mouse monoclonal, dilution 1:500, Sigma-Aldrich) for 18 h at 4 °C. Secondary antibodies were either anti-rabbit IgG antibodies or anti-mouse IgG antibodies (BioRad, USA, Sigma-Aldrich, respectively) conjugated to HRP. The chromogen used was 3,3′-diaminobenzidine (DAB) dissolved in Tris-NaCl buffer (pH 7.5). Finally, sections were counterstained with Gill's haematoxylin, dehydrated and processed as described previously. For negative control staining, incubation with primary antibody was omitted. The morphometric analysis of positively stained cells was done at 1000 magnification using Olympus Microscope B×51 and a Digital Analysis Imaging system „Analysis Docu" (Soft Imaging Systems 3.0, Prague, CR). The number of immunoreactive (IR) cells in the peripheral, central areas and inflammatory lesions were finally calculated for 0.1 mm^2 after recording in an average 30 screen fields per area on the sections of tumors from 4 mice.

2.10.3. Detection of apoptosis using TUNEL technique

Another set of paraffin sections was subjected to TUNEL technique which is based on the detection of fragmented DNA in the cells undergoing apoptosis. TUNEL staining included following steps. Briefly, deparaffinised and rehydrated sections were incubated for 15 min at 42 °C with proteinase K diluted in 10 mM Tris-HCl at the final concentration of 20 μg/ml followed by three washing steps. Blocking of endogenous peroxidase activity was performed for 30 min at RT during immersion of slides in PBS containing 2% H_2O_2. Washed sections were pre-incubated for 10 min at RT with TdT buffer in the humidified chamber and then were covered with staining solution containing 4 μl (120 U) of TdT transferase (Promega) and 4 μl of 16-dUTP-biotin (4 nmol) [50] per 1 ml of TdT buffer. Staining reaction was carried out at 37 °C for 2 h and stopped by replacing of staining solution with TB buffer for 15 min at RT. In negative control staining, TdT transferase was omitted. After repeated washing in PBS, sections were incubated in streptavidin-HRP [50] solution (2% BSA in PBS, pH 7.2) at dilution of 1:300 for 1 h at 22 °C. DAB was used as an enzymatic substrate and sections were counterstained with Gill's haematoxylin as described above.

2.11. Malondialdehyde determination

Lipid peroxidation in the liver tissue was determined by the modified method of Mihara and Uchiyama [35], which is based on the reaction of malondialdehyde (MDA) with thiobarbituric acid forming product that has absorption maximum at 530 nm with 1,1,3,3-tetraethoxypropane used as a standard for MDA. Malondialdehyde is one of many low molecular weight end-products of lipid hydroperoxide decomposition and is most often used as an index of lipid peroxidation. Lipid peroxidation expressed in μmoles MDA/g proteins was determined in the liver samples in triplicates ($n = 10$) during each experiment. Cell proteins were determined in the liver homogenates by the Lowry protein assay, using BSA (Sigma-Aldrich) as a protein standard.

2.12. Statistical analysis

Each value from *in vitro* experiments represents the mean ± SD of three independent experiments performed in duplicates and the mean and standard deviation for each value was calculated. Results were analyzed using one-way ANOVA followed by Tukey's post -hoc test for comparisons with control. In the grouped analyses, two-way ANOVA and Bonferoni post-hoc test were applied. All data were analyzed with GraphPad Prism Software (version 5) (GraphPad Software).

3. Results

3.1. Total number of 4T1 and NMuMG cells and its clonogenic potential

Total cell number of mouse breast carcinoma 4T1 cells decreased after ATR therapy in time- and concentration dependent manner with a significant decline after the incubation with 50 and 75 μM of ATR (Fig. 1A). In normal mouse mammary epithelial NMuMG cells the similar results with less pronounced decrease of the cell number after ATR therapy was found (Fig. 1B). Concentration of DMSO used for ATR dissolution (less than 0.1% in each ATR concentration tested) had no effect on the total cell number of both 4T1 as well as NMuMG cells (data not shown). Clonogenic potential of cancer 4T1 cells was not affected by 25 and 50 μM concentration of ATR and only 75 μM ATR significantly reduced clonogenic ability of 4T1 cell line when compared with untreated control (Fig. 1C). On the other hand, clonogenicity of NMuMG cells was not affected by any of ATR concentrations tested (Fig. 1D). Based on this result, we can conclude that carcinoma cells 4T1 are more sensitive to ATR therapy then normal epithelial NMuMG cells.

3.2. Cell cycle distribution and BrdU incorporation in 4T1 cells

No significant differences in the cell cycle distribution were observed between 4T1 and NMuMG cells after 24–72 h of ATR treatment (Fig. 2A, B). Results of the cell cycle analysis indicate that ATR treatment did not lead to the significant interference with DNA integrity and/or cell division (accumulation of cells in some phase of the cell cycle) of 4T1 as well as NMuMG cells. We present the result from 72 h time point only (Fig. 2A, B). Based on results of the clonogenic assay as well as the cell cycle analysis of 4T1 cells, we

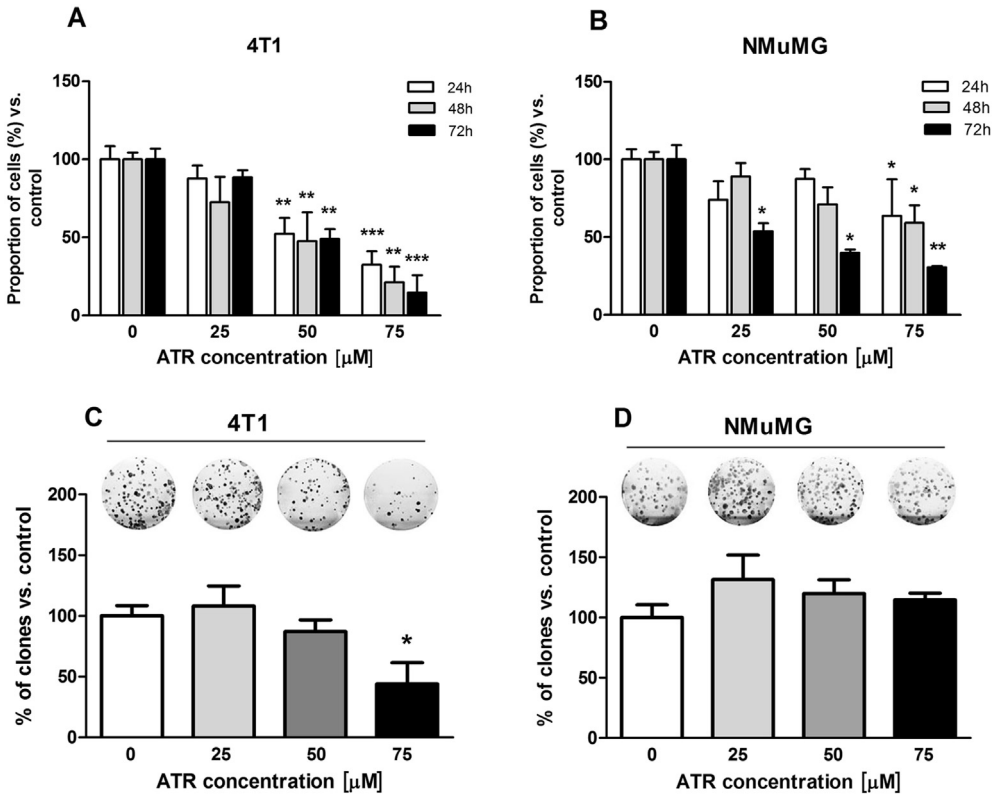

Fig. 1. The number and the clonogenic ability of 4T1 and NMuMG cells after atranorin therapy. 4T1 (A) and NMuMG (B) cells were treated with atranorin (25, 50 or 75 μM) for 24, 48 or 72 h and then collected and counted in Bürker chamber. For clonogenic assay: 4T1 (C) and NMuMG (D) cells were treated with atranorin (25, 50 or 75 μM) for 24 h and after re-counting seeded onto six-well plates in density of 1000 viable cells per well in complete media and followed by cultivation for another 8–10 days. At the end the cells were fixed and stained with methylene-blue. The data are presented as mean ± SD of three independent experiments. The statistical significance is designated as follows: atranorin vs. control as *($p < 0.05$); **($p < 0.01$) and ***($p < 0.001$).

decided to test BrdU incorporation into DNA of these cells after ATR exposure. Interestingly, BrdU incorporation was not affected neither by 50 μM, or 100 μM of ATR and only the highest concentration (150 μM) significantly declined BrdU incorporation into 4T1 cells (Fig. 2C). These results correlate well with decrease in the total number of 4T1 cells. Therefore we assume that decreased BrdU incorporation in 4T1 cells after incubation with the highest ATR concentration is a false positive result induced by the direct cytotoxic and/or apoptotic effect of ATR rather than by anti-proliferative one.

3.3. Caspases activity and western blot of 4T1 cells

The application of 25 or 50 μM concentrations of ATR increased caspase-3 and caspase-like proteases activity in cancer 4T1 cells within 1 h period. The same concentrations of ATR induced more pronounced increase of caspase activity in 4T1 cells later on, to be exact between 3 and 6 h time points (Fig. 3A). Indeed, there was a significant difference in caspase activation after ATR between 4T1 and NMuMG cells. In this regard, cancer 4T1 cells revealed 5–6 fold increase of caspase-3 and caspase-like proteases activity compared to the untreated control. ATR-treated normal NMuMG cells reached only 1–1.8 fold increase of caspase activity later, after 3 h period (Fig. 3B). Vehicle-treated cancer cells as well as normal cells did not show any caspase activity changes when compared with control cells (data not shown). Furthermore, ATR therapy induced clear PARP protein cleavage in cancer 4T1 cells already at 24 h time point. In spite of the absence of PARP cleavage in NMuMG cells at 24 h period, prolonged ATR treatment (48 h) did reveal PARP cleavage in these cells. ATR treatment moderately increased anti-apoptotic Bcl-x_L protein levels in 4T1 cells at 24 h time point, meanwhile depletion of Bcl-x_L protein was demonstrated after 48 h of incubation with ATR. In contrast, there were only nonsignificant changes of Bcl-x_L protein levels in NMuMG cells after ATR treatment (Fig. 3C).

Pro-apoptotic Bax protein expression was very low in 4T1 untreated cells and ATR increased Bax level after exposure to 50 μM concentration within 24 h, and maintaining this level of expression for further 24 h. On the other hand, Bax protein level decreased in normal NMuMG cells after incubation with ATR at the concentrations of 25 and 50 μM at 24 h time point. Prolonged exposure of NMuMG cells (48 h) to ATR caused a significant increase of Bax expression (Fig. 3C). Interestingly, Hsp90 protein level was up-regulated in 4T1 cells after 50 μM of ATR at 48 h, but remained unchanged in normal NMuMG cells at the same time point (Fig. 3C).

3.4. Survival of 4T1 tumor-bearing mice following therapy, tumor volumes and, weights

Following inoculation of 2.5×10^5 of 4T1 cells into mammary gland of Balb/c mice, first tumors appeared on day 4 and enlarged continuously. ATR was administered to mice orally in ten daily doses representing in total 300 mg/kg of body weight per mouse. As presented by Kaplan-Meier curve (Fig. 4A) survival period in group of ATR-treated mice was significantly prolonged ($P = 0.0147$). The mean survival time in the control and treated group was 9.6 and 17.3 days, respectively and the median (median survival) was between 5 and 20 days, respectively. Next day following the

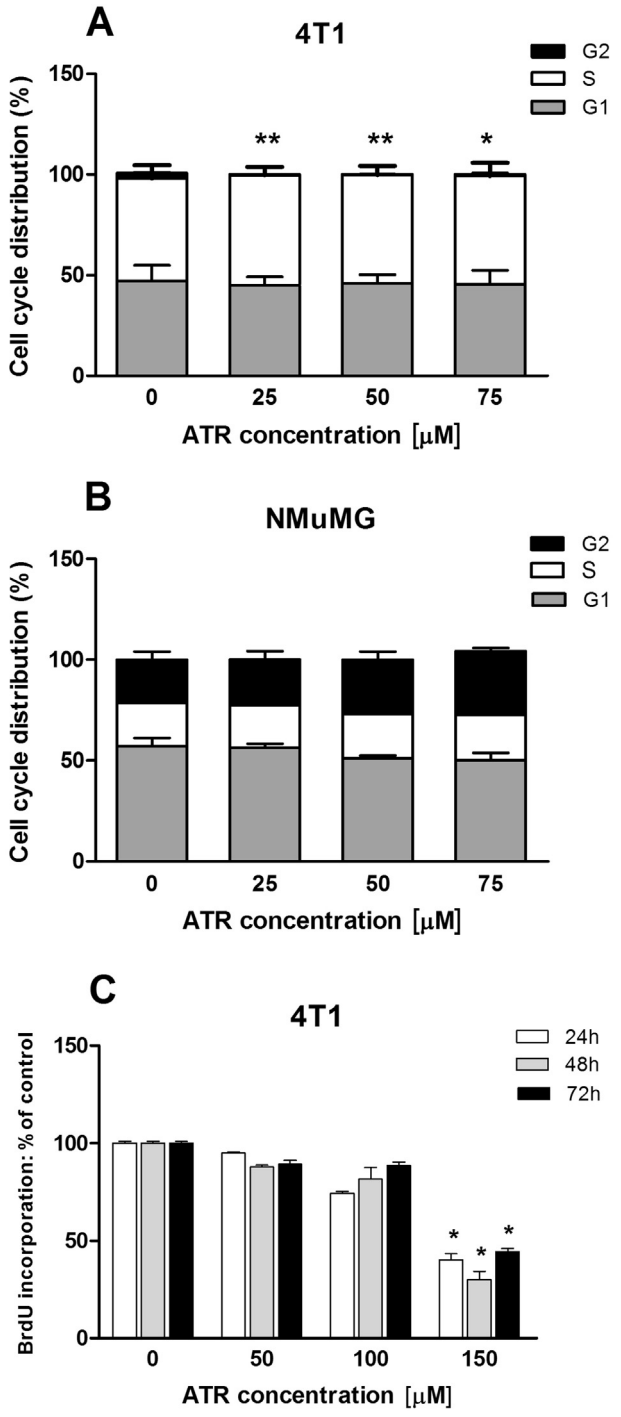

Fig. 2. The cell cyle distribution of 4T1 and NMuMG cells and the proliferation of 4T1 cells after atranorin therapy. 4T1 (A) and NMuMG (B) cells were treated with atranorin (25, 50 or 75 μM) for 72 h and then fixed with 70% ethanol, labelled with propidium iodide and evaluated by flow cytometry (FACSCalibur, Becton Dickinson, CA, USA). The data indicates the percentage of 15,000 events of cells in indicated phase of the cell cycle. For the BrdU incorporation: 4T1 (C) cells were treated with atranorin (50, 100 or 150 μM) for 24, 48 or 72 h and analyzed by ELISA proliferation kit [50] according to the manufacturer's protocol. Data are presented as a mean ± SD of three independent experiments. The statistical significance is designated as follows: atranorin vs. control as *($p < 0.05$; **($p < 0.01$); ***($p < 0.001$).

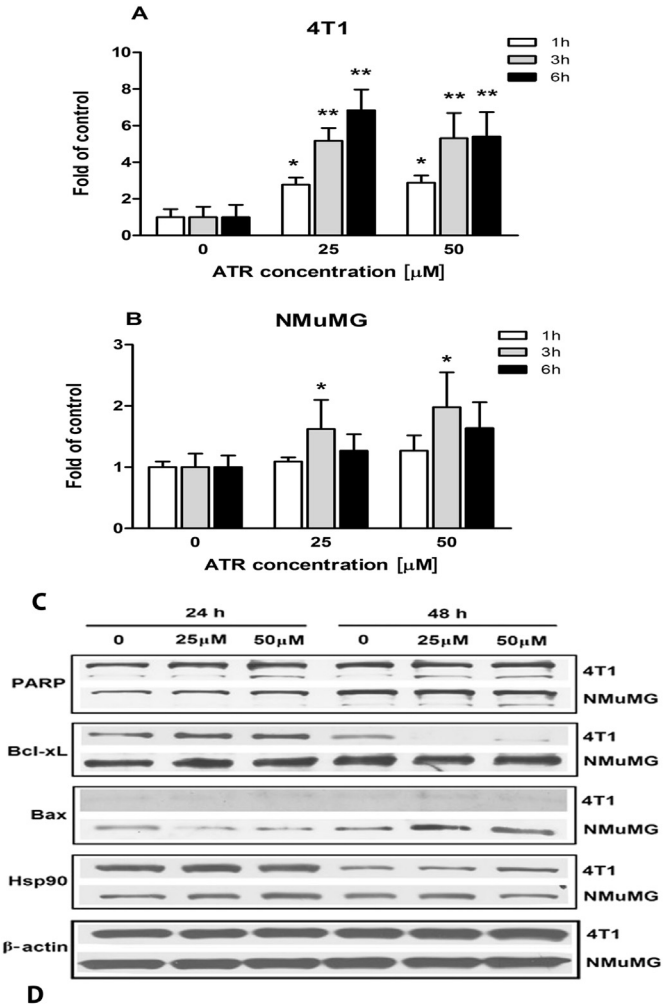

D

		24 h			48 h		
Cell Line	Protein	Control	25 μM	50 μM	Control	25 μM	50 μM
4T1	*Bcl-Xl*	1.0±0.2	1.5±0.4	1.4±0.3	1.0±0.1	0.1±0.02**	0.2±0.03**
NMuMG		1.0±0.1	1.1±0.2	1.5±0.4	1.0±0.3	0.9±0.1	1.1±0.2
4T1	*Bax*	1.0±0.1	1.5±0.5	2.4±0.3**	1.0±0.2	2.6±0.2*	2.9±0.3***
NMuMG		1.0±0.3	0.5±0.2	0.6±0.3	1.0±0.2	2.2±0.3**	1.8±0.2*
4T1	*Hsp90*	1.0±0.2	1.1±0.3	1±0.2	1.0±0.1	1.3±0.4	2.6±0.3**
NMuMG		1.0±0.1	1.2±0.4	1.6±0.2*	1.0±0.2	1.1±0.2	0.7±0.2

Fig. 3. Caspase-3 activation and the response of PARP, Bcl-X_L, Bax, and Hsp90 proteins in both 4T1 and NMuMG cells after atranorin therapy. 4T1 (A) and NMuMG (B) cells were treated with ATR (25 or 50 μM) for 1, 3 or 6 h and caspase activity was analyzed according to the manufacturer's protocol (see Materials and methods). The caspases activities are depicted as folds of untreated control. For the western blots: 4T1 and NMuMG cells (C) were lysed after 24 or 48 h atranorin therapy (25 or 50 μM). Equal amounts of protein extracts were resolved on 12% SDS-PAGE and analyzed by western blot. Each blot is representative of three independent experiments with β-actin used as a loading control. The relative amounts (densitometric levels) of proteins were normalized to the corresponding levels of β -actin in each line (D). The data are presented as mean ± SD of three independent experiments. The statistical significance is designated as follows: atranorin vs. control as *($p < 0.05$), **($p < 0.01$) and *** ($p < 0.001$).

termination of therapy tumors were isolated and volumes (Fig. 4B) and weights (Fig. 4C) were determined. While ATR therapy significantly reduced tumor volumes in comparison with untreated mice ($P = 0.0021$), weights of tumors were reduced only slightly ($P = 0.200$).

3.5. Tumor morphology and 4T1 cells proliferation in vivo

Paraffin sections stained with classical Mayer's haematoxylin/

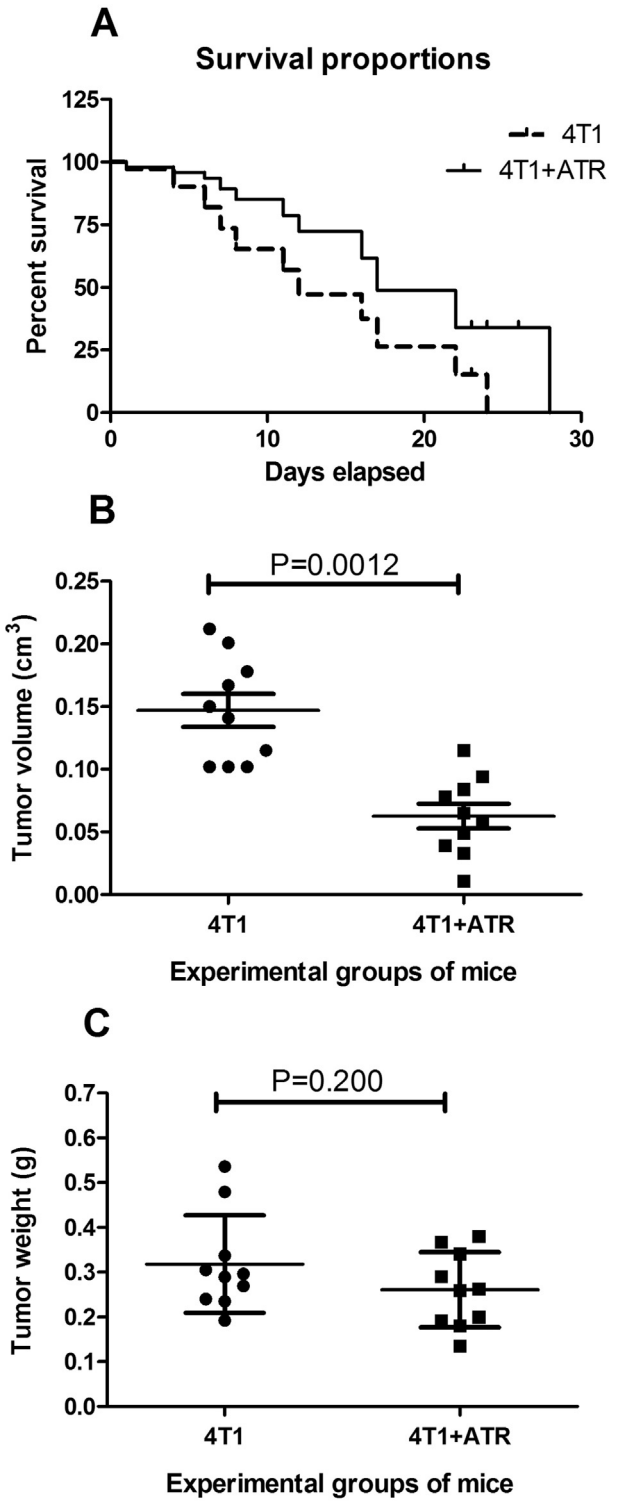

Fig. 4. Effects of atranorin on survival of mice, tumor volumes and weights. The female of BALB/c mice were inoculated at the age of 10 weeks with 250,000 4T1 cells/animal and ATR was administered orally at the concentration of 30 mg/kg body weight daily for 10 days starting from fourth day after 4T1 cell inoculation. Survival periods of mice in control and treated groups of mice are shown by Kaplan–Meier curve (A). Volumes (B) and weights (C) of tumors from control (4T1) group and ATR-treated (4T1+ATR) group of mice was determined on the first day post therapy.

eosin staining allowed to compare the basic morphological characteristics of tumor tissue. Tumors from both groups of mice shared the same characteristic such as presence of stroma formed by collagen fibres (Fig. 5A), vascularisation, sporadic ducts and adipose cells. However, in tumors from treated mice, inflammatory lesions with apoptotic/necrotic cells and blood leakage (Fig. 5B) occupied larger areas and fibrotic stroma seemed to be more developed. These differences might shed more light on the discrepancies between reduction in tumor weight and volume. To assess whether ATR interfered with proliferative capacity of 4T1 cells, mice received i.p. injection of BrdU and the marker incorporated into nuclei of tumors was detected on frozen sections. As shown on Fig. 5C (4T1, untreated) and Fig. 5D (4T1+ATR), distribution of FITC-labelled nuclei appeared to be very similar.

3.6. Apoptosis of 4T1 cells in tumors

In several *in vitro* tests we have demonstrated that ATR has pro-apoptotic effect at significantly lower concentrations in 4T1 cells than in NMuMG cells. To test whether ATR in its parent formulation can induce apoptosis in 4T1 cells in tumors after oral administration, we evaluated the expression of Bax as opposite to Bcl-x_L proteins as well as TUNEL-positive cells on paraffin sections. In tumors from untreated mice, 4T1 cells positive for Bax protein, were very scarce (not shown). Following ATR therapy, Bax-immunoreactivity (IR) was often detected in proliferating cells and in cells with fragmented nuclei, thus indicating a late apoptosis (Fig. 6A–B). Notably, cells undergoing apoptosis were accumulated in the inflammatory lesions (Fig. 6C). Data from morphometric analyses showing significantly elevated numbers of apoptotic 4T1 cells in all three tumor areas (peripheral, 16.30 ± 2.17; central, 12.85 ± 1.96 and lesions, 40.61 ± 5.93, resp.) in ATR-treated mice comparing to control group are summarized on Fig. 6D. Bcl-x_L immunoreactivity was very rare in tumors from both groups and was seen sporadically in proliferating 4T1 cells (not shown) indicating activation of self-protecting process in 4T1 cells.

To verify the pro-apoptotic effect of ATR *in vivo*, we performed the specific TUNEL staining of nuclei with fragmented DNA, what coincides with the early phase of apoptosis. In accordance with previously shown data, positively stained nuclei of 4T1 cells were detected in significantly higher numbers in all three areas (Fig. 6E) in comparison to controls. However the mean counts were lower (6.13 ± 1.7, 4.21 ± 0.84 and 10.97 ± 2.18). A very few apoptotic nuclei appeared in the tumors from untreated mice (Fig. 6F). Elevated numbers were recorded in the inflammatory lesions (Fig. 6G) and peripheral areas (Fig. 6H) of tumors from treated mice.

3.7. Hepatoprotective and antioxidant activity of ATR in mice

The hepatocytes are very sensitive cells to the damage by drugs and xenobiotics and the assessment of biological activities of compounds should include *in vivo* examination of their hepatotoxicity on animal models. Hepatocytes respond to the physiological and metabolic damage by imbalance between reactive oxygen species (ROS) and cellular antioxidant systems resulting in ROS overproduction, what causes lipid peroxidation. Moreover, host-inflammatory response during oncological diseases is associated with oxidative stress in the tissues infiltrated by tumor-derived cancer cells [16,31]. Livers from intact ATR-treated or untreated control as well as from 4T1-tumor bearing and ATR-treated or untreated mice were subjected to biochemical determination of lipid peroxides. As shown on Fig. 7, the administration of ATR significantly decreased MDA concentration ($P < 0.01$) in ATR-treated 4T1-tumor bearing mice (μmol of MDA/g of proteins) compared to 4T1 control animals (6.49 ± 0.414 vs. 4.84 ± 0.253). Low levels of lipid peroxidation were detected also in the intact mice (3.70 ± 0.38) and were diminished significantly ($P < 0.05$)

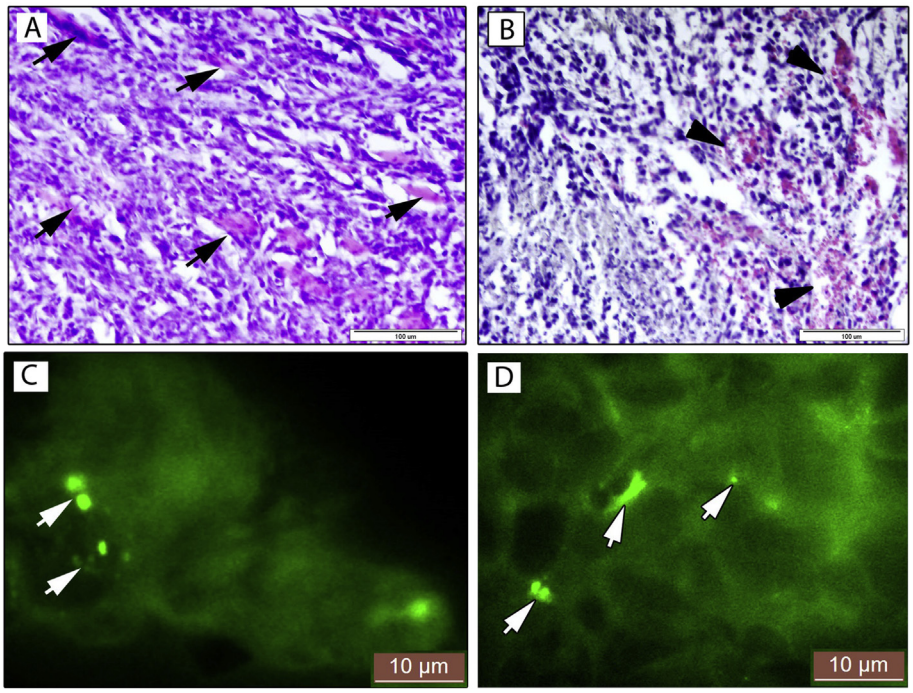

Fig. 5. Tumor morphology and 4T1 cells proliferation *in vivo*. Tumors from control (4T1) and treated mice (4T1+ATR) embedded in paraffin sections were cut and stained with Mayer's haematoxylin/eosin. In tumors from ATR-treated groups a fibrotic stroma was more developed (A) and inflammatory lesions with apoptotic/necrotic cells and blood leakage (B) occupied larger areas. Immunofluorescent localization of proliferating 4T1 cells in the frozen tumors sections appeared to be very similar with control (C) and ATR-treated mice (D). Mice in both groups received an i.p. injections of BrdU (n = 4) and the nuclei with incorporated marker were visualized with anti-BrdU-FITC antibody.

after ATR administration, suggesting a direct antioxidant and hepatoprotective effect of ATR *in vivo*.

4. Discussion

Usnic acid came from a comparison of anti-tumor effect of six lichen secondary metabolites (diffractaic acid, lobaric acid, usnic acid, vicanicin, variolaric acid, and protolichesterinic acid) towards three human cancer cell lines MCF-7, HeLa and HCT-116 tested as the most effective metabolite [9]. In this regard, Brisdelli et al. [9] revealed the involvement of caspase-3, −8, and −9 in the programmed cell death induced by protolichesterinic acid in HeLa cells. Another *in vitro* studies indicate that orcinol derivatives of tenuiorin isolated from the lichen *Peltigera leucophlebia* and lichen metabolites sphaerophorin, pannarin, and epiphorellic acid-1 inhibit the growth of pancreatic and colon cancer cell lines as well as human prostate carcinoma cells (DU-145), respectively [26]. Furthermore, sphaerophorin, pannarin, and epiphorellic acid-1 induced apoptosis in DU-145 cells through the increase of caspase-3 enzyme activity, high DNA fragmentation, but without the disruption of the plasma membrane [44].

Since a lack of information on the exact mechanism of lichen secondary metabolites action on cancer cells, Bačkorová et al. [1,2] attempted to shed more light on this issue when focussed on lichen acids as activators of programmed cell death, acting probably through the mitochondrial pathway in A2780 and HT-29 cancer cell lines. In this regard, Bačkorová et al. [2] have found that usnic acid and ATR are more effective anti-cancer compounds when compared with parietin and gyrophoric acid. This fact was partly confirmed by Russo et al. [46] who showed that ATR at high concentrations was able to affect moderately “cellular vitality“ (a metabolic activity determined by MTT assay) of prostate cancer cells. Although ATR inhibited metabolic activity of prostate cancer cells after 72 h incubation at concentrations of 25 and 50 μM, it did not show any effect on the release of lactate dehydrogenase, or on the activity of caspase-3 as well as the expression of Bax and Bcl-2 proteins in prostate cancer cells [46]. This is in contrast to Bačkorová et al. [2], who demonstrated that ATR and usnic acid induce apoptosis in human A2780 and HT-29 cancer cells via massive loss in the mitochondrial membrane potential together with caspase-3 activation (observed only in HT-29 cells) and phosphatidylserine externalization. The authors also detected an increased induction of both ROS and RNS shortly after the administration of secondary metabolites, which could be a part of the cytotoxic action of lichen metabolites [2]. Our experimental model also confirmed ATR-induced apoptosis demonstrated by an early increased of caspase-3 activity, clear PARP cleavage and the depletion of Bcl-x_L protein. In the contrary to Bačkorova et al. [2], elevation of Bax protein expression *in vitro* was more significant in cancer 4T1 cells than normal NMuMG cells. Moreover, our *in vivo* model confirmed that ATR induced apoptosis in 4T1 cells as seen in tumor tissue by DNA fragmentation and also increased Bax protein levels.

Antitumor effect of the secondary lichen metabolites may be mediated by the direct induction of apoptosis as well as by their antiproliferative activity. Regarding the proliferation, ATR and usnic acid proved to inhibit cell proliferation (MTT assay) in almost all tested human cancer cell lines [1]. On the contrary, ATR did not show any anti-proliferative effect, recorded as thymidine uptake, on human breast T47D, pancreatic Panc-1 and prostate PC-3 cancer cell lines but other metabolites, namely usnic acid [27] together with protolichesterinic acid and lobaric acid [21], interfered with proliferation of all above mentioned cells. In our study we did not confirm anti-proliferative effect of ATR on 4T1 cells (BrdU incorporation) *in vitro* and *in vivo*. The discrepancies in ATR effect on the proliferation of cancer cells could be explained by different methodology and/or sensitivity of assay as well as by different purity of ATR used. In this regard, although secondary metabolite parietin

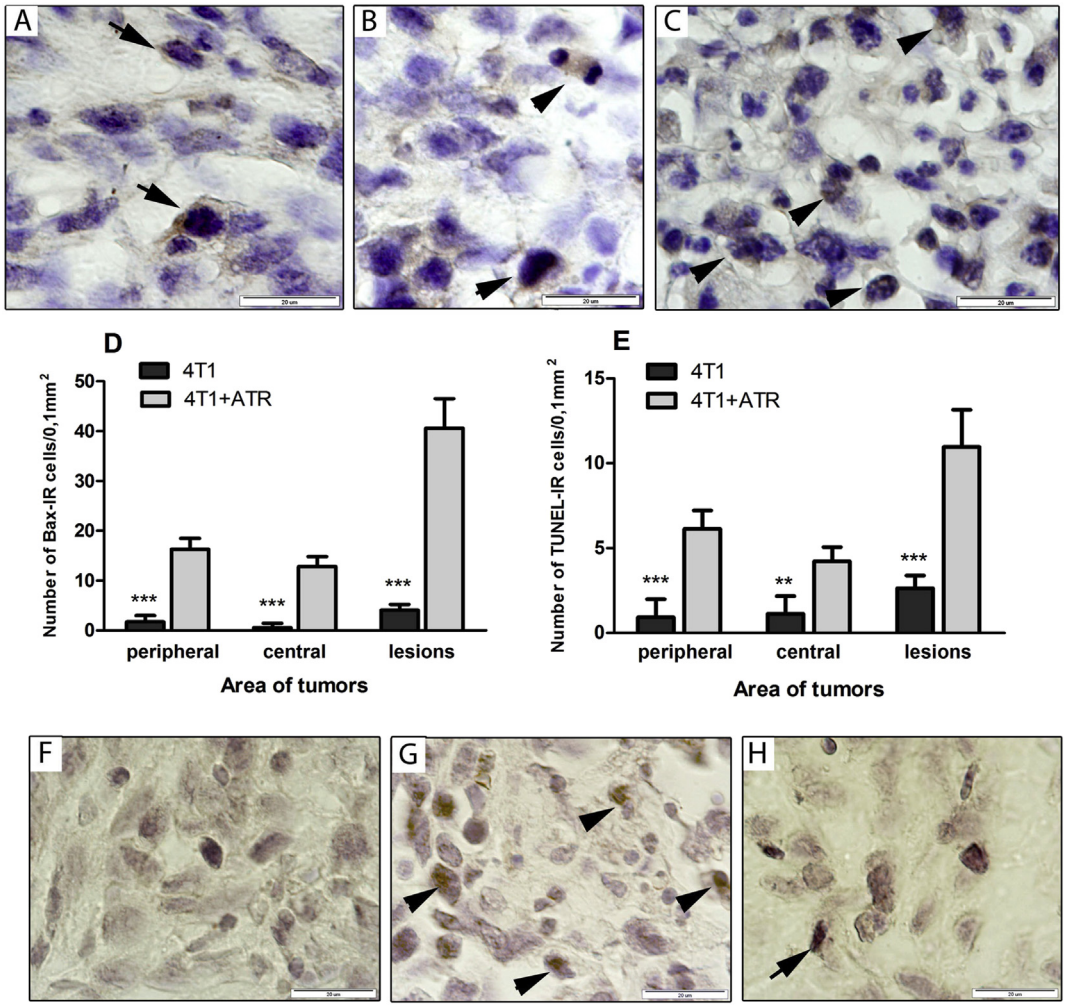

Fig. 6. Apoptosis of 4T1 cells in tumors. Detection of cells expressing markers of apoptotic process was performed by immunohistochemical localization of pro-apoptotic protein Bax. Localization of fragmented DNA in the cells undergoing apoptosis was done by TUNEL method on tumors paraffin sections. (A–C), representative microphotographs of sections showing Bax expression in 4T1 cells seen as dark brown colour (dark arrows). Immunoreactive cells (IR) in the central area (A) and peripheral area (B) also involved proliferating cells (arrowhead). IR-cells in inflammatory area (C) often contained fragmented (late apoptosis) nuclei (arrowheads). Morphometric analysis of Bax-IR cells (D) and TUNEL-positive cells (E) in three morphological areas of tumors revealed pro-apoptotic effect of ATR in 4T1-derived tumors. TUNEL-positive cells were very rare in tumors from control mice (F), and their number increased in the inflammatory lesions (Fig. 6G) and peripheral areas (Fig. 6H) in tumors from treated mice. The statistical significance is designated as follows: ATR-treated vs. control as $^{**}p < 0.01$, $^{***}p < 0.001$. (For interpretation of the references to colour in this figure legend, the reader is referred to the web version of this article.)

isolated from lichen *Xanthoria parietina* did not reveal anti-proliferative activity on human breast cancer cells, whole extract inhibited proliferation accompanied by modulation of p16, p27, cyclin D1 and cyclin A genes expression [4]. Another explanation for diverse effects of ATR and other secondary metabolites of lichens on the proliferation of cancer cells could be high concentration of DMSO used as a solvent of secondary metabolites. Bačkorova et al. [1,2] used DMSO as solvent but the effect of DMSO alone at the concentration higher than 0.5%, in tested metabolite solutions, was not observed.

The generation of free radicals *in vivo* is a constant phenomenon due to either physiological metabolism or pathological alterations. ROS, as toxic byproducts of oxygen metabolism, can have deleterious effects on macromolecules, including cell lipids [20]. Nowadays, there are divergent results concerning the concentration of lipid peroxidation products in tumors of different origins [3] and very little is known about this process in tissues other than the tumor in the tumor-bearing organisms unaffected by any therapy. Although the concentration of lipid peroxidation products in cells did not always correlate with the level of oxidative stress, lipid peroxidation is a common denominator of oxidative stress caused by peroxide, superoxide, UV, heat and oxidant chemicals such as doxorubicin [3]. It was shown, that usnic acid at high dose can induce loss of cell membrane integrity in isolated normal rat hepatocytes by increasing the release of cellular transaminases, increasing lipid peroxidation and aniline hydroxylase activity and decreasing glutathione content [42]. On the other hand, ATR possesses a redox active potential *in vitro*, acting as a pro-oxidant or antioxidant agent depending on the type of radical and its concentration [34]. Although ATR increased lipid peroxidation induced by thermolysis of 2, 20-azo-bis (2-amidinopropane) dihydrochloride, it protected SH-SY5Y cells against H_2O_2 induced cytotoxicity [34]. On the other hand, the extracts from lichen *Toninia candida* containing also ATR exhibited strong antioxidant activity, DPPH and hydroxyl radical scavenging and chelating activity and also inhibitory activity towards lipid peroxidation *in vitro* [30]. 4T1 cells are highly metastatic cell line, infiltrating also livers in the tumor bearing mice [22]. We suppose that metastatic liver foci and associated inflammation contributed to the oxidative stress and lipid peroxidation as detected by increased MDA levels. In our study

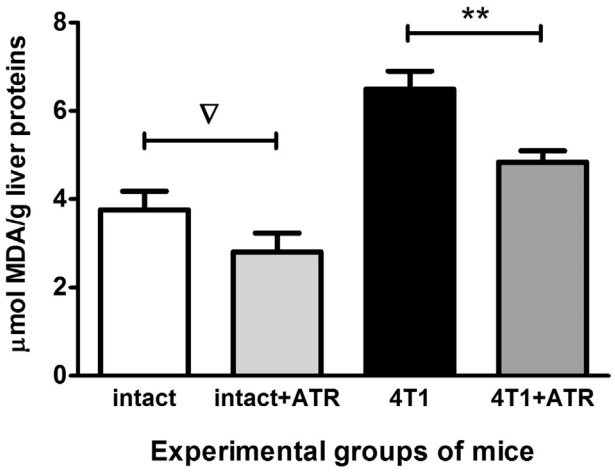

Fig. 7. The effect of atranorin on hepatic lipid peroxidation of mice. Intensity of lipid peroxidation in the livers of untreated (intact) and ATR-treated control (intact + ATR) as well as untreated (4T1) and ATR-treated 4T1 tumor bearing mice (4T1-ATR). Lipid peroxidation was determined on the first day post therapy and is expressed as a concentration of malondialdehyde (MDA; µmoles MDA/g proteins). Data represent means ± SD for each data set. The statistical significance is designated as follows: intact + ATR vs. intact as ▼ $p < 0.05$ and 4T1+ATR vs. 4T1 as $^{**}p < 0.01$.

ATR did not show any hepatotoxicity and significantly diminished amount of lipid peroxides in the liver of intact mice, probably due to its direct antioxidant activity. Similarly, treatment of 4T1 tumor-bearing mice with ATR profoundly reduced lipid peroxidation as a results of ROS-scavenging activity. Although not examined, the reduction of metastatic foci in the liver following therapy by reported pro-apoptotic activity could also contributed to reduced liver pathology. Based on our best knowledge, we demonstrated for the first time a selective and/or stronger cytotoxic effect of ATR on cancer cells compared to normal livers *in vivo*. Similarly we corroborate the diverse response of ATR on cancer 4T1 cells in comparison with normal NMuMG cells *in vitro*. Furthermore, we point out that ATR mediated inhibition of lipid peroxidation *in vivo* in the livers of intact mice as well as inhibition of lipid peroxidation in the livers of tumor-bearing mice when compared to the untreated tumor bearing controls.

5. Conclusions

ATR induced apoptosis of mouse mammary carcinoma 4T1 cells *in vitro* and *in vivo* rather than having antiproliferative effect. On the contrary, normal mammary epithelial NMuMG cells were less sensitive to ATR therapy *in vitro*. Furthermore, our studies revealed for the first time the hepatoprotective effect of ATR against lipid peroxidation in liver cells of *in vivo* mouse mammary carcinoma model.

Conflict of interest

"The authors declare no conflict of interest".

Acknowledgment

This study was supported by the Scientific Grant Agency of the Ministry of Education of the Slovak Republic under contract Nos. VEGA 1/0394/15 and VEGA 2/0150/13.

Transparency document

Transparency document related to this article can be found online at http://dx.doi.org/10.1016/j.cbi.2016.03.012.

References

[1] M. Backorova, M. Backor, J. Mikes, R. Jendzelovsky, P. Fedorocko, Variable responses of different human cancer cells to the lichen compounds parietin, atranorin, usnic acid and gyrophoric acid, Toxicol. Vitro 25 (2011) 37–44.
[2] M. Backorova, R. Jendzelovsky, M. Kello, M. Backor, J. Mikes, P. Fedorocko, Lichen secondary metabolites are responsible for induction of apoptosis in HT-29 and A2780 human cancer cell lines, Toxicol. Vitro 26 (2012) 462–468.
[3] G. Barrera, Oxidative stress and lipid peroxidation products in cancer progression and therapy, ISRN Oncol. 2012 (2012) 137289.
[4] A. Basile, D. Rigano, S. Loppi, A. Di Santi, A. Nebbioso, S. Sorbo, et al., Antiproliferative, antibacterial and antifungal activity of the lichen Xanthoria parietina and its secondary metabolite parietin, Int. J. Mol. Sci. 16 (2015) 7861–7875.
[5] M.A. Bazin, A.C. Le Lamer, J.G. Delcros, I. Rouaud, P. Uriac, J. Boustie, et al., Synthesis and cytotoxic activities of usnic acid derivatives, Bioorg. Med. Chem. 16 (2008) 6860–6866.
[6] C. Bezivin, S. Tomasi, I. Rouaud, J.G. Delcros, J. Boustie, Cytotoxic activity of compounds from the lichen: Cladonia convoluta, Planta Med. 70 (2004) 874–877.
[7] M. Blanch, Y. Blanco, B. Fontaniella, M.E. Legaz, C. Vicente, Production of phenolics by immobilized cells of the lichen Pseudevernia furfuracea: the role of epiphytic bacteria, Int. Microbiol. 4 (2001) 89–92.
[8] D. Bogo, M.F. de Matos, N.K. Honda, E.C. Pontes, P.M. Oguma, E.C. da Santos, et al., In vitro antitumour activity of orsellinates, Z. Naturforsch. C 65 (2010) 43–48.
[9] F. Brisdelli, M. Perilli, D. Sellitri, M. Piovano, J.A. Garbarino, M. Nicoletti, et al., Cytotoxic activity and antioxidant capacity of purified lichen metabolites: an in vitro study, Phytother. Res. 27 (2013) 431–437.
[10] T.S. Bugni, C.D. Andjelic, A.R. Pole, P. Rai, C.M. Ireland, L.R. Barrows, Biologically active components of a Papua New Guinea analgesic and anti-inflammatory lichen preparation, Fitoterapia 80 (2009) 270–273.
[11] B. Burlando, E. Ranzato, A. Volante, G. Appendino, F. Pollastro, L. Verotta, Antiproliferative effects on tumour cells and promotion of keratinocyte wound healing by different lichen compounds, Planta Med. 75 (2009) 607–613.
[12] I.Z. Carlos, M.B. Quilles, C.B. Carli, D.C. Maia, F.P. Benzatti, T.I. Lopes, et al., Lichen metabolites modulate hydrogen peroxide and nitric oxide in mouse macrophages, Z. Naturforsch. C 64 (2009) 664–672.
[13] P.A. Cohen, J.B. Hudson, G.H. Towers, Antiviral activities of anthraquinones, bianthrones and hypericin derivatives from lichens, Experientia 52 (1996) 180–183.
[14] E.R. Correche, R.D. Enriz, M. Piovano, J. Garbarino, M.J. Gomez-Lechon, Cytotoxic and apoptotic effects on hepatocytes of secondary metabolites obtained from lichens, Altern. Lab. Anim. 32 (2004) 605–615.
[15] M.G. De Carvalho, G.J.A. De Carvalho, R. Braz-Filho, Chemical constituents from Ouratea floribunda: complete H-1 and C-13 NMR assignments of atranorin and its new acetyl derivative, J. Braz. Chem. Soc. 11 (2000) 143–147.
[16] S.A. DuPre, D. Redelman, K.W. Hunter Jr., The mouse mammary carcinoma 4T1: characterization of the cellular landscape of primary tumours and metastatic tumour foci, Int. J. Exp. Pathol. 88 (2007) 351–360.
[17] E. Einarsdottir, J. Groeneweg, G.G. Bjornsdottir, G. Harethardottir, S. Omarsdottir, K. Ingolfsdottir, et al., Cellular mechanisms of the anticancer effects of the lichen compound usnic acid, Planta Med. 76 (2010) 969–974.
[18] A. Falk, T.K. Green, P. Barboza, Quantitative determination of secondary metabolites in Cladina stellaris and other lichens by micellar electrokinetic chromatography, J. Chromatogr. A 1182 (2008) 141–144.
[19] M. Garcez, D.D. Melo, A. Antunes, D.S. Araújo, M.R. Serafini, L.F. Carvalho, Anti-inflammatory and Toxicity Studies of Atranorin Extracted from Cladina Kalbii Ahti in Rodents, 2011, p. 47.
[20] L. Gate, J. Paul, G.N. Ba, K.D. Tew, H. Tapiero, Oxidative stress induced in pathologies: the role of antioxidants, Biomed. Pharmacother. 53 (1999) 169–180.
[21] S. Haraldsdottir, E. Guolaugsdottir, K. Ingolfsdottir, H.M. Ogmundsdottir, Antiproliferative effects of lichen-derived lipoxygenase inhibitors on twelve human cancer cell lines of different tissue origin in vitro, Planta Med. 70 (2004) 1098–1100.
[22] G.H. Heppner, F.R. Miller, P.M. Shekhar, Nontransgenic models of breast cancer, Breast Cancer Res. 2 (2000) 331–334.
[23] K. Hirabayashi, S. Iwata, M. Ito, S. Shigeta, T. Narui, T. Mori, et al., Inhibitory effect of a lichen polysaccharide sulfate, GE-3-S, on the replication of human immunodeficiency virus (HIV) in vitro, Chem. Pharm. Bull. (Tokyo) 37 (1989) 2410–2412.
[24] N.K. Honda, F.R. Pavan, R.G. Coelho, S.R. de Andrade Leite, A.C. Micheletti, T.I. Lopes, et al., Antimycobacterial activity of lichen substances, Phytomedicine 17 (2010) 328–332.
[25] K. Ingolfsdottir, G.A. Chung, V.G. Skulason, S.R. Gissurarson, M. Vilhelmsdottir, Antimycobacterial activity of lichen metabolites in vitro, Eur. J. Pharm. Sci. 6 (1998) 141–144.
[26] K. Ingolfsdottir, G.F. Gudmundsdottir, H.M. Ogmundsdottir, K. Paulus, S. Haraldsdottir, H. Kristinsson, et al., Effects of tenuiorin and methyl orsellinate from the lichen Peltigera leucophlebia on 5-/15-lipoxygenases and

proliferation of malignant cell lines in vitro, Phytomedicine 9 (2002) 654–658.
[27] T. Kristmundsdottir, E. Jonsdottir, H.M. Ogmundsdottir, K. Ingolfsdottir, Solubilization of poorly soluble lichen metabolites for biological testing on cell lines, Eur. J. Pharm. Sci. 24 (2005) 539–543.
[28] Y. Liu, D.V. Messadi, H. Wu, S. Hu, Oral lichen planus is a unique disease model for studying chronic inflammation and oral cancer, Med. Hypotheses 75 (2010) 492–494.
[29] M.B. de Sousa Maia, N.H. da Silva, E.F. da Silva, M.T.J. Catanho, A.R.P. Schuler, E.C. Pereira, Antinociceptive activity of crude extracts and atranorin obtained from the lichen Cladina dendroides (des Abb.) Ahti, Acta Farm, Bonaer 21 (2002) 259–264.
[30] N.T. Manojlovic, P.J. Vasiljevic, P.Z. Maskovic, M. Juskovic, G. Bogdanovic-Dusanovic, Chemical composition, antioxidant, and antimicrobial activities of lichen Umbilicaria cylindrica (L.) Delise (Umbilicariaceae), Evid. Based Complement. Altern. Med. 2012 (2012) 452431.
[31] J.M. Mates, J.A. Segura, F.J. Alonso, J. Marquez, Oxidative stress in apoptosis and cancer: an update, Arch. Toxicol. 86 (2012) 1649–1665.
[32] M. Mayer, M.A. O'Neill, K.E. Murray, N.S. Santos-Magalhaes, A.M. Carneiro-Leao, A.M. Thompson, et al., Usnic acid: a non-genotoxic compound with anticancer properties, Anticancer Drugs 16 (2005) 805–809.
[33] M.G. Melo, A.A. Araujo, C.P. Rocha, E.M. Almeida, S. Siqueira Rde, L.R. Bonjardim, et al., Purification, physicochemical properties, thermal analysis and antinociceptive effect of atranorin extracted from Cladina kalbii, Biol. Pharm. Bull. 31 (2008) 1977–1980.
[34] M.G. Melo, J.P. dos Santos, M.R. Serafini, F.F. Caregnato, M.A. Pasquali, T.K. Rabelo, et al., Redox properties and cytoprotective actions of atranorin, a lichen secondary metabolite, Toxicol. Vitro 25 (2011) 462–468.
[35] M. Mihara, M. Uchiyama, Determination of malonaldehyde precursor in tissues by thiobarbituric acid test, Anal. Biochem. 86 (1978) 271–278.
[36] P.L. Nimis, N. Skert, Lichen chemistry and selective grazing by the coleopteran Lasioderma serricorne, Environ. Exp. Bot. 55 (2004) 175–182.
[37] M. Niyazi, I. Niyazi, C. Belka, Counting colonies of clonogenic assays by using densitometric software, Radiat. Oncol. 2 (2007) 4.
[38] L.J.-T. Nybakken, Riitta. UV-B induces usnic acid in reindeer lichens, Lichenologist 38 (2006) 477–485.
[39] M.A. O'Neill, M. Mayer, K.E. Murray, H.M. Rolim-Santos, N.S. Santos-Magalhaes, A.M. Thompson, et al., Does usnic acid affect microtubules in human cancer cells? Braz. J. Biol. 70 (2010) 659–664.
[40] H.M. Ogmundsdottir, G.M. Zoega, S.R. Gissurarson, K. Ingolfsdottir, Anti-proliferative effects of lichen-derived inhibitors of 5-lipoxygenase on malignant cell-lines and mitogen-stimulated lymphocytes, J. Pharm. Pharmacol. 50 (1998) 107–115.
[41] H. Pöykkö, M. Hyvärinen, M. Bačkor, Removal of lichen secondary metabolites affects food choice and survival of Lichenivorous Moth Larvae, Ecology 86 (2005) 2623–2632.
[42] P. Pramyothin, W. Janthasoot, N. Pongnimitprasert, S. Phrukudom, N. Ruangrungsi, Hepatotoxic effect of (+)usnic acid from Usnea siamensis Wainio in rats, isolated rat hepatocytes and isolated rat liver mitochondria, J. Ethnopharmacol. 90 (2004) 381–387.
[43] B. Proksa, J. Adamcova, M. Sturdikova, J. Fuska, Metabolites of Pseudevernia furfuracea (L.) Zopf. and their inhibition potential of proteolytic enzymes, Pharmazie 49 (1994) 282–283.
[44] A. Russo, M. Piovano, L. Lombardo, L. Vanella, V. Cardile, J. Garbarino, Pannarin inhibits cell growth and induces cell death in human prostate carcinoma DU-145 cells, Anticancer Drugs 17 (2006) 1163–1169.
[45] A. Russo, M. Piovano, L. Lombardo, J. Garbarino, V. Cardile, Lichen metabolites prevent UV light and nitric oxide-mediated plasmid DNA damage and induce apoptosis in human melanoma cells, Life Sci. 83 (2008) 468–474.
[46] A. Russo, S. Caggia, M. Piovano, J. Garbarino, V. Cardile, Effect of vicanicin and protolichesterinic acid on human prostate cancer cells: role of Hsp70 protein, Chem. Biol. Interact. 195 (2012) 1–10.
[47] R.S. Siqueira, L.R. Bonjardim, A.A. Araujo, B.E. Araujo, M.G. Melo, M.G. Oliveira, et al., Antinociceptive activity of atranorin in mice orofacial nociception tests, Z. Naturforsch. C 65 (2010) 551–561.
[48] P. Solar, M. Chytilova, Z. Solarova, J. Mojzis, P. Ferenc, P. Fedorocko, Photodynamic therapy with hypericin improved by targeting HSP90 associated proteins, Pharmaceuticals 4 (2011) 1488–1502.
[49] K.A. Solhaug, P. Larsson, Y. Gauslaa, Light screening in lichen cortices can be quantified by chlorophyll fluorescence techniques for both reflecting and absorbing pigments, Planta 231 (2010) 1003–1011.
[50] S.A. Susin, H.K. Lorenzo, N. Zamzami, I. Marzo, B.E. Snow, G.M. Brothers, et al., Molecular characterization of mitochondrial apoptosis-inducing factor, Nature 397 (1999) 441–446.
[51] M. Takai, Y. Uehara, J.A. Beisler, Usnic acid derivatives as potential antineoplastic agents, J. Med. Chem. 22 (1979) 1380–1384.
[52] T. Tokiwano, H. Satoh, T. Obara, H. Hirota, Y. Yoshizawa, Y. Yamamoto, A lichen substance as an antiproliferative compound against HL-60 human leukemia cells: 16-O-acetyl-leucotylic acid isolated from Myelochroa aurulenta, Biosci. Biotechnol. Biochem. 73 (2009) 2525–2527.
[53] N. Valencia-Islas, A. Zambrano, J.L. Rojas, Ozone reactivity and free radical scavenging behavior of phenolic secondary metabolites in lichens exposed to chronic oxidant air pollution from Mexico City, J. Chem. Ecol. 33 (2007) 1619–1634.
[54] K.O. Vartia, On antibiotic effects of lichens and lichen substances, Ann. Med. Exp. Biol. Fenn. 28 (1950) 1–82.
[55] M. Yilmaz, A.O. Turk, T. Tay, M. Kivanc, The antimicrobial activity of extracts of the lichen Cladonia foliacea and its (-)-usnic acid, atranorin, and fumarprotocetraric acid constituents, Z Naturforsch. C 59 (2004) 249–254.